PRAMANA
— journal of
physics

© Printed in India

Vol. 48, No. 4,
April 1997
pp. 937–950

Resonance de-enhancement in the 2^1A_g state of *trans*-azobenzene

NANDITA BISWAS and SIVA UMAPATHY*
Department of Inorganic and Physical Chemistry, Indian Institute of Science, Bangalore 560012, India
*Author to whom correspondence should be addressed
Email: umapathy @ ipc.iisc.ernet.in

MS received 20 August 1996; revised 2 December 1996

Abstract. We analyze the origin of de-enhancement for a number of vibrational modes in the 2^1A_g excited state of *trans*-azobenzene. We have used the time-dependent wave packet analysis of the RR intensities by including the multimode damping effects in the calculation. This avoids the use of unrealistically large values for the damping parameter. It is concluded that the de-enhancement is caused by the interference between the two uncoupled electronic states, and that the intensities observed under the so-called symmetry forbidden $2^1A_g \leftarrow 1^1A_g$ transition are purely due to resonance excitation. It is also observed that the use of the time-dependent approach to study the de-enhancement effects caused by multiple electronic states on the RR intensities is not necessarily useful if one is interested in the structural dynamics.

Keywords. Resonance Raman intensities; de-enhancement; time-dependent wave-packet analysis; *trans*-azobenzene.

PACS No. 33·20

1. Introduction

Resonance Raman (RR) intensities observed at different excitation wavelengths, termed the Raman excitation profiles (REPs), can be used to infer structure and dynamics in the resonant excited state [1–3]. In general, REPs provide information on the vibrational mode-dependent dynamics, in contrast to an absorption spectrum, which contains information on all the vibrational modes associated with that particular transition. Thus, RR intensities have been utilized constructively, through modeling and simulation, to relate to the distortions in the excited state of a given vibrational mode [1–4]. However, the intensities observed experimentally are occasionally far less than expected under resonance excitation, which has been ascribed to de-enhancement effects [4–18].

Raman intensity is proportional to the modulus square of transition polarizability ($\alpha_{f\leftarrow i}$), which is given by Kramers–Heisenberg–Dirac (KHD) expression [19, 20] and depends on the electronic transition moment (M), the vibrational overlap factors and the energy difference between the incident laser light and the energy gap between ground and excited electronic levels. Assuming very small dependence of M on the

nuclear coordinate Q, it can be expanded in Taylor's series about the ground state equilibrium geometry (Q_0). Thus

$$M(Q) = M_0 + \sum_j (\partial M/\partial q_j)_0 q_j + 1/2 \sum_{j,k} (\partial^2 M/\partial q_j \partial q_k)_0 q_j q_k + \cdots. \tag{1}$$

The first term M_0 which is independent of the nuclear coordinate Q has maximum contribution to the Franck–Condon (A') term of the transition polarizability under resonance excitation. Thus, the vibrations that are totally symmetric can be strongly A'-term enhanced, only when there is significant distortion upon electronic excitation which leads to considerable values for the vibrational overlap integrals. A'-term gains importance only when resonance is approached and thus implicitly depends on nuclear coordinate displacement.

Due to the explicit dependence of M on Q (i.e. the first order term in (1)), vibronic coupling may occur within the same electronic state s (viz. $\langle s|h_a|s\rangle$, where $h_a \equiv (\delta H/\delta Q_a)Q_0$ is the coupling operator and the subscript a refers to the normal mode. This gives rise to the A term contribution to the transition polarizability or, between two different electronic states e and s (viz. $\langle s|h_a|e\rangle$ i.e. B term contribution to the transition polarizability). A and B terms are important when incident energy is off-resonant from a particular electronic state.

The origin of de-enhancement in the REPs is well documented [9, 14, 16, 21] as due to the interference from an electronic state other than the resonant excited state. However, the modelling of these effects depends very much on such factors as the energy difference between the resonant and interfering state, the transition moments of the two electronic states, nature (spin state, symmetry and polarization) of the two states involved and the vibronic coupling between them. The A and B terms arising due to vibronic coupling may interfere with the strongly resonant (Franck–Condon) A'-term of the polarizability tensor to give an anti-resonance effect in the REP of a totally symmetric vibration. This approach has been utilized successfully for a number of systems [4–7, 9]. Another plausible explanation of the observed de-enhancement is the interference between the resonant scattering A'-terms of $\alpha_{f\leftarrow i}$ from two different electronic states e (the resonant state) and s (the interfering state). When the scattering tensor $\alpha_{f\leftarrow i}$ contains contributions from A'_e (i.e. the resonant electronic state 'e') and A'_s (viz. the pre-resonant state 's'), the RR intensity (I_R) is proportional to the product of the scattering tensors $\alpha_{f\leftarrow i}$ and its complex conjugate, i.e.

$$I_R \propto \alpha_{f\leftarrow i} \alpha^*_{f\leftarrow i} \tag{2a}$$

or

$$I_R \propto (A'_{res} + A'_{pre})(A'^*_{res} + A'^*_{pre}) \tag{2b}$$

or

$$I_R \propto |A'_e|^2 + |A'_s|^2 + A'_e A'^*_s + A'_s A'^*_e. \tag{2c}$$

Thus, destructive or constructive interference may occur depending on the sign and relative magnitude of the respective polarizability terms [9(a), 16].

Recently, a time-dependent wave packet dynamical approach has been presented by Shin and Zink [16], taking into consideration the correlation functions of two excited electronic states. Here, the effects of changes in displacements, transition dipole moments of both the excited electronic states and the influence of Γ on the REPs have

been studied. This approach is based on Heller's wave packet formalism [22], which provides an intuitive physical picture for the de-enhancement process. However, Zink's approach deals with individual modes and therefore involves large damping constants [16]. In this paper we have utilized a similar approach to study the REPs of *trans*-azobenzene (TAB) but included a multi-mode damping parameter, such that the damping factor used is more realistic than the earlier values. We find that the time-dependent approach is very effective in predicting the origin of de-enhancement.

TAB absorption spectrum exhibits a lowest energy symmetry forbidden ($2^1A_g \leftarrow 1^1A_g$) transition with unusually large absorption coefficient, in addition to the strongly allowed ($1^1A_u \leftarrow 1^1A_g$) transition [21]. As a result, TAB undergoes isomerization via two different mechanisms, depending on the excitation wavelength [23–25]. In an earlier paper [25] we have modelled the REPs of ten totally symmetric (polarized) fundamentals recorded under the $2^1A_g \leftarrow 1^1A_g$ transition, using Heller's wavepacket formalism. A comparison of the simulated REPs with experimental results shows that only five out of ten vibrational modes fit very well with the experimental results. The other five modes have structure in the REPs, thus deviating considerably from the theoretically predicted profiles [25]. Further, the experimental REPs are expected to follow the shape of the absorption spectrum if the intensities observed are purely due to resonant excitation [1, 26, 27]. But in TAB, the experimetal REPs for a few vibrational modes at 1439, 1312, 1181, 1142 and 1000 cm^{-1} show a decrease in Raman intensity near the maximum of $2^1A_g \leftarrow 1^1A_g$ absorption band.

In this paper, we have analyzed the REPs of TAB using Zink's approach [16] and find that the experimental profile can be successfully simulated if the influence of an additional electronic state is taken into account. In particular, we have addressed the question of using Zink's approach to studying the resonance de-enhancement for polyatomic systems, where mode-dependent dynamics is different in the two interfering states. This is an important question considering that the earlier studies [16] based on this approach have assumed the ratio of vibrational displacements to be the same in the two electronic states. Maintaining the ratio of displacements will only be valid, if the Raman intensities retain the same ratio among all the modes of interest in the two electronic states (which is rarely the case in most systems).

Further, a comparative study of the results obtained from two-mode as well as multi-mode calculations is presented. These results show that the de-enhancement is caused by interference between two uncoupled excited electronic surfaces and the simulated values of displacements obtained from multi-mode calculations lead to valuable clues regarding the extent of contribution of a given vibration to the dynamics involved, on excitation.

2. Theory and computational methods

Resonance Raman intensities can be calculated using either the sum over states [28, 29] or the time-dependent method [22]. In the time-dependent picture, the Raman amplitude for the transition from the initial state $|i\rangle$ to the final state $|f\rangle$ (where both the vibrational eigenstates $|i\rangle$ and $|f\rangle$ correspond to the electronic ground state) is expressed as a half Fourier transform of the Raman correlation function $\langle f|i(t)\rangle$,

$$\alpha_{f\leftarrow i}(E_L) = \frac{i}{\hbar}\int_0^\infty M^2 \langle f|i(t)\rangle \exp\left[i\frac{(E_L+E_i)t}{\hbar} - \frac{\Gamma t}{\hbar}\right]dt, \tag{3}$$

where, E_i the zero point energy of the ground electronic state, E_L the energy of the incident photon, M the electronic transition dipole moment, and Γ the phenomenological line width parameter, $\hbar = h/2\pi$ (h being Planck's constant), and $|i(t)\rangle$ is the evolving wavepacket at various intervals of time, i.e,

$$|i(t)\rangle = \exp\left(-\frac{iH_{ex}t}{\hbar}\right)|i\rangle, \tag{4}$$

where, H_{ex} is the excited state Hamiltonian. The Raman intensity can thus be related to the polarizability as folllows

$$I_R \propto E_L E_S^3 |\alpha_{f\leftarrow i}|^2 \tag{5}$$

where, E_S is the energy of the scattered photon.

The autocorrelation $\langle i|i(t)\rangle$ and the Raman correlation function $\langle f|i(t)\rangle$ are computed using the extended Simpson's rule [30, 33] from the time-evolving wavepacket $|i(t)\rangle$. The full Fourier transform of the former gives the absorption spectrum, and the half Fourier transform of the latter gives the REP. Thus, when there is only one excited electronic state, the expression for polarizability ($\alpha_{f\leftarrow i}$) in the time-domain (eq. (3)) holds good. But when we consider two excited electronic states, interfering and resonant states, the Raman correlation functions are computed separately, multiplied by the square of the respective transition dipole moments and then summed up to give the total correlation function. The half Fourier transform of the total Raman correlation function gives the final expression for the polarizability ($\alpha_{f\leftarrow i}$) in a two state model.

$$\alpha_{f\leftarrow i}(E_L) = \frac{i}{\hbar}\int_0^\infty (M_R^2 O_R + M_I^2 O_I)\exp\left[i\frac{(E_L + E_i)t}{\hbar} - \frac{\Gamma t}{\hbar}\right]dt, \tag{6}$$

where M_R and M_I are the transition dipole moments and O_R and O_I are the Raman correlation functions of the resonant and interfering excited electronic states respectively. From this expression, it is seen that the factors which influence the polarizability are (i) the relative transition dipole moments of the resonant and interfering excited electronic states (since $\alpha_{f\leftarrow i}$ is related to the square of the transition dipole moment, the state having the largest transition dipole moment may dominate the REPs), (ii) the displacement (Δ) of the excited potential surfaces from the minimum of the ground state along the normal modes, and (iii) the damping factor Γ.

The de-enhancement phenomenon observed in TAB has been systematically studied using the above approach. In particular, all those factors which significantly influence the RR intensities have been critically considered. Both two mode and multi-mode calculations have been carried out and a comparative picture is presented in §3. In the absence of Duschinsky mixing, the multi-mode Raman correlation function is given as the product of correlation function $\langle f_k|i_k(t)\rangle$ for the Raman active mode (k) and the autocorrelation function $\langle i_j|i_j(t)\rangle$ for the rest of the vibrational modes (j).

$$\langle f|i(t)\rangle_M = \langle f_k|i_k(t)\rangle \prod_{j=1,j\neq k}^{N-1} \langle i_j|i_j(t)\rangle, \tag{7}$$

where N is the total number of vibrational modes present. The polarizability $\alpha_{f\leftarrow i}$ for the multi-mode calculataions can be obtained by substituting the value of $\langle f|i(t)\rangle_M$ in (6).

Using (3) where the evolution of the wavepacket is carried out with the grid technique [30–32], a model calculation was done for a two-mode system in order to test the validity of our computational method. The fitting parameters used here are exactly the same as those used in Zink's model [16]. The frequencies of two modes are 500 and 700 cm^{-1} respectively. The zero-zero energies for the resonant (E^{R}_{00}) and the interfering (E^{I}_{00}) excited electronic states are 20 000 cm^{-1} and 30 000 cm^{-1}. The dimensionless displacement (Δ) is 1·0 for the two modes in both the excited electronic states. The value of the homogeneous broadening (Γ) is 700 cm^{-1}, and the ratio of the squares of the transition dipole moments in the two electronic states (M_R^2/M_I^2) is 1/60. The simulated real and imaginary parts of $\alpha_{f\leftarrow i}$ for the two electronic states are shown in figure 1 (a), and the REPs for three cases when (*i*) $M_I = 0$, (ii) $M_R^2/M_I^2 = 1/30$ and (iii) $M_R^2/M_I^2 = 1/60$ are shown in figure 1(b). These results are consistent with the literature data [16] confirming our computational algorithm.

3. Results and discussion

The absorption spectrum and the REPs of all the ten Raman active vibrational modes of TAB under the symmetry forbidden ($2^1A_g \leftarrow 1^1A_g$) transition (assuming a point

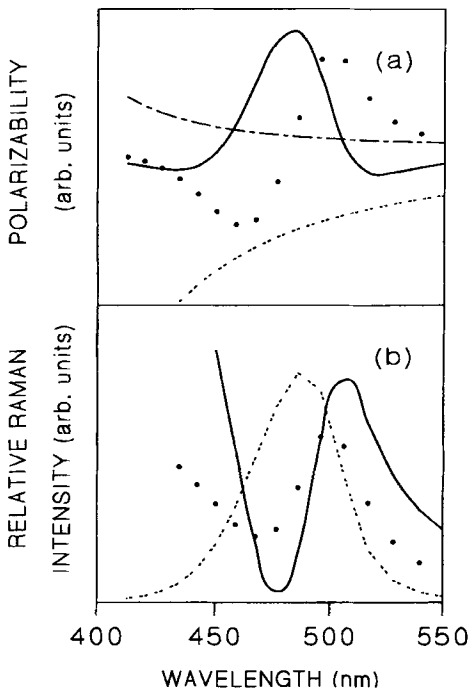

Figure 1. **(a)** Real and imaginary parts of the polarizability (α) for two electronic states. Real (..... resonant state, and –·–·– interfering state) and imaginary (—— resonant state and ------- interfering electronic state) parts for the 700 cm^{-1} mode when $M_R^2/M_I^2 = 1/60$. **(b)** Resonance Raman excitation profiles for the 700 cm^{-1} mode when (i) $M_I = 0$ (------), (ii) $M_R^2/M_I^2 = 1/30$ (.....) and, (iii) $M_R^2/M_I^2 = 1/60$ (——). The displacements are 1.0 for the modes and $\Gamma = 700$ cm^{-1} in both excited states. $E^{R}_{00} = 20000$ cm^{-1} and $E^{I}_{00} = 30000$ cm^{-1}.

group of C_i symmetry [34]) was simulated on a single excited potential energy surface [25]. Since the low temperature absorption spectrum of TAB does not show any vibrational structure in the visible region, we have considered the short time dynamics to analyze the RR intensities. For systems undergoing short-time dynamics it is assumed that the resonance Raman intensities (I_R) of the normal modes are

$$I_R \propto \Delta^2 \omega^2, \tag{8}$$

where Δ and ω are the dimensionless displacement of the excited electronic state with respect to the ground state and the frequency for the normal coordinate in cm^{-1} respectively. Also, the TAB absorption spectrum as well as Raman spectrum is insensitive to solvent effects. As a result, the effect of solvent induced broadening function has not been taken into consideration.

REPs of various vibrational modes of TAB in resonance with the absorption band of $2^1A_g \leftarrow 1^1A_g$ transition have been calculated [25] using this time-dependent approach assuming (a) all the potential energy surfaces are harmonic except the torsional mode which is considered to be linear and dissociative in the excited electronic state, (b) the normal coordinates are not mixed in the excited state (no Duschinsky effect), (c) the transition dipole moments are constant, and (d) the frequencies for all the vibrational modes are the same in both ground and excited electronic states. The propagation of the wavepacket on the excited electronic surface has been carried out using the time-dependent quantum-mechanical (TDQM) method involving a grid technique [30–32]. The REPs, as shown in figure 4 of [25] did not fit the experimental data accurately for five of the vibrational modes. In all these cases the experimental REPs show structure with an inflexion near the absorption spectral maximum and a peak towards the higher wavelength.

In order to account for the possibilities of the structure in REPs of five totally symmetric modes of TAB, we have measured (i) the positions of the peak maximum and that of the dip, (ii) the full width at half maximum (FWHM) of the peak as well as the full width at half depth (FWHD) of the dip and these are given in table 1 for the respective modes.

First concentrating on the occurrence of the peak, it is found that the position of the peak maximum is about 478–516 nm (see table 1). As observed earlier by Rimai *et al* [15(a)] for naphthalene, the peak positions in REPs could correspond to a dipole forbidden transition. In their study, Rimai *et al* concluded that the peak observed was

Table 1. Trans-azobenzene Raman frequencies (ω in cm^{-1}), position of the dip and the peak in the REPs of the modes undergoing de-enhancement and their FWHM.

Frequency (ω cm^{-1})	Position of dip (nm)	FWHD of dip (cm^{-1})	Point of peak (nm)	FWHM of peak (cm^{-1})
1439	458	–	478	–
1312	441	2098	516	4775
1181	441	2304	496	2449
1142	441	2070	497	2850
1000	465	2446	512	2486

due to a triplet state since the phosphorescence peak maximum matched with that of the REP peak. Similarly, in TAB, excited states inaccessible by an electric dipole transition may be considered responsible for the peak maximum in the REPs. In fact, Monti *et al* [35] have predicted, from *ab initio* calculations that the presence of a dipole forbidden state with an E_{00} value of 591·3 nm. but, as shown in table 1, the peak maxima for these vibrations are at $\sim 478-516$ nm and the FWHM of the peak is $\sim 60-70$ nm for most of the modes, with the exception of 1312 cm^{-1} (FWHM ~ 130 nm). Therefore, it is unlikely that a dipole forbidden state is responsible for the structure observed in the REPs. Moreover, no experimental evidence for the presence of a triplet state in TAB has been reported so far, which provides further justification for discarding the presence of a dipole forbidden state as a probable reason for the peak observed in REPs.

Next we consider the inflexion observed in the REPs, which can be attributed to resonance de-enhancement. The loss of RR intensity can be ascribed either to (a) destructive interference between the real or imaginary parts of the polarizability of two nearby electronic states or, (b) population interference [17] (curve crossing) between the resonant and the nearby electronic states.

In the case of (a), the relative magnitude of interference on the observed polarizability mainly depends on (i) the energy difference, (ii) individual vibrational mode displacements and (iii) transition dipole moments of the interfering and resonant electronic states. In the case of (b), specific signatures in the experimentally observed REPs provide clues to the existence of curve crossing. In particular, it has been suggested [17] that the width at half depth (FWHD) of the de-enhanced REP is expected to be of the order of one vibrational quantum and the de-enhancement minimum of the resonant REP occurs near the energy at which the two potential energy curves cross. The FWHD and the wavelength at which the lowest RR intensity is observed for all the Raman active vibrations of TAB are given in table 1 First, the width at half depth of the de-enhanced REPs, in our case, is obviously not of the order of one vibrational quantum. Secondly, the lowest intensity is observed at or near the peak maximum (~ 441 nm) of the electronic absorption spectrum, which is more an indication of destructive interference of polarizability tensors of the two electronic states [16, 17] (*vide infra*). Thus, occurrence of population interference due to curve crossing is unlikely and it seems reasonable to conclude that the de-enhancement must originate from a destructive interference induced by a state close to the resonant electronic state.

The origin of de-enhancement in the case of (a) occurs when either (i) both the interfering and resonant electronic excited states are well separated in energy ($\sim 10\,000$ cm^{-1}) and the transition dipole moment (M_I) for the interfering state is much higher than the transition dipole moment (M_R) for the resonant electronic state, or, (ii) both the interfering and resonant electronic excited states are close in energy (~ 1000 cm^{-1}) and the values of M_I and M_R are comparable. Both (i) and (ii) can be explained in terms of destructive interference of the imaginary parts of the polarizability ($\alpha_{f\leftarrow i}$). In the previously studied examples [16] it is found that this kind of interference due to the imaginary parts leads to a minimum in the REPs at wavelengths near the maximum of the resonant absorption band, as observed in this study on TAB.

In addition, in the case of TAB there are no electronic states close to the ($2^1A_g \leftarrow 1^1A_g$) transition with similar transition dipole moment values. Rather, a state

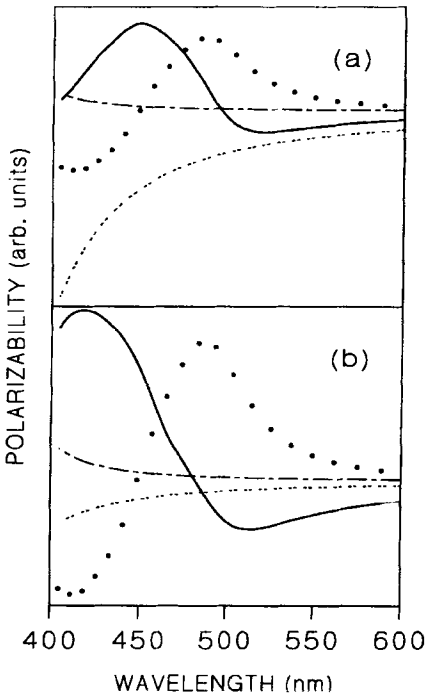

Figure 2. Real and imaginary parts of the polarizability (α) for two electronic states. Real (..... resonant state, — - — interfering state) and imaginary (—— resonant state and ------ interfering electronic state) parts for **(a)** 1181 cm^{-1} mode and **(b)** 1491 cm^{-1} mode when $M_R = 0{\cdot}8$Å and $M_I = 2{\cdot}52$Å. Δ_1 and Δ_2 for both 1181 cm^{-1} and 1491 cm^{-1} modes are given in table 3. E^R_{00} and E^I_{00} are 20470 cm^{-1} and 27710 cm^{-1} respectively and $\Gamma = 1200$ cm^{-1} for both excited states.

corresponding to the $(1^1A_u \leftarrow 1^1A_g)$ transition is present, that is well separated in energy from the resonant electronic transition and that has a much higher value of the transition dipole moment. Also, unsuccessful attempts were made to fit the experimental REPs by considering the presence of a dipole forbidden state (*vide supra*) lying close to the resonant electronic state with similar transition probabilities. Thus, in the present study, we find that the possibility of interference between $(2^1A_g \leftarrow 1^1A_g)$ and $(1^1A_u \leftarrow 1^1A_g)$ transitions are most probable.

The REPs for the ring H rock ($\omega = 1181$ cm^{-1}) and ring stretch ($\omega = 1491$ cm^{-1}) of TAB in resonance with the $(2^1A_g \leftarrow 1^1A_g)$ transition and interference from $(1^1A_u \leftarrow 1^1A_g)$ transition have been simulated, first, by taking only these two modes into consideration. These two modes (1181 exhibiting de-enhancement and 1491 with no de-enhancement in the experimental REPs) were specifically chosen to test the validity of the use of two mode calculations as has been successfully carried out earlier [16] for other systems. The zero-zero energies (E^R_{00} and E^I_{00}) for the first and the second electronic states and the transition dipole moments (M_R and M_I) which were obtained from the absorption spectrum are 20470 cm^{-1} and 27710 cm^{-1} and 0·8Å and 2·52 Å, respectively. Results obtained from the two mode calculations are shown in figures 2

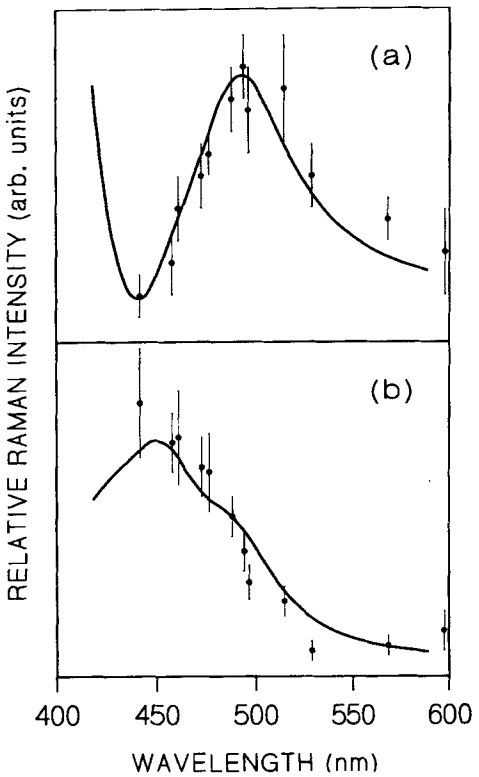

Figure 3. REPs for **(a)** 1181 cm^{-1} mode and **(b)** 1491 cm^{-1} mode obtained from two-mode calculations. Solid lines are the simulated curves and dotted line with error bar shows the experimental curve.

and 3. In figures 2(a) and 2(b), the real and imaginary parts of the polarizability tensor for the two vibrational modes are shown. These simulations required large damping parameters ($\Gamma \sim 1200\ cm^{-1}$). Initially, the values of dimensionless displacements of the two modes are estimated from the experimental RR intensities under the resonant electronic state, which after successive iterations give the best possible displacements (Δ) that can reproduce the experimental REPs for the respective modes. The best fit dimensionless displacements Δ_1 and Δ_2 are 1·5 and 1·45 for 1181 cm^{-1} (Δ_1 and Δ_2 for the 1491 cm^{-1} mode being 0·67 and 0·15) for figure 3(a) and 2·0 and 0·15 for 1491 cm^{-1} (Δ_1 and Δ_2 for the 1181 cm^{-1} mode being 0·67 and 1·45) for figure 3(b). Large Δ_2 values result in strong de-enhancement, whereas small Δ_2 values give no de-enhancement in the REPs. Also, small Δ_1 values give low FWHM for the peak and the position of reduced intensity is observed at higher wavelengths. The reverse is true for large Δ_1 values. A strong anti-resonance effect is observed near the absorption maximum of the symmetry forbidden transition in 1181 cm^{-1} (figure 3(a)). This is because of destructive interference between the imaginary parts of the polarizability tensor ($\alpha_{f\leftarrow i}$) for the two excited electronic states. The imaginary parts of both resonant and interfering states have comparable magnitudes and are opposite in sign near the maxima of the first

electronic transition ($\sim$ 441 nm) (figure 2a), and as a result, they interfere destructively giving rise to reduced intensity at that position. Since the magnitude of the imaginary part of $(\alpha_{f\leftarrow i})$ for the interfering electronic state, 1491 cm^{-1}, is negligible in comparison to that of the resonant electronic state (figure 2(b)), the REP for the 1491 cm^{-1} mode (figure 3(b)) is dominated by the polarizability of the latter electronic state, and hence no interference effect is seen in this case. These figures clearly demonstrate the effect of Δ_1 and Δ_2 on the REPs of TAB, as was shown previously by Zink *et al* [16] for a model system. An important point to note is that it has been possible to maintain the ratio of the displacements (i.e. not consistent with experimental RR intensities) of the two modes in order to match the simulated REPs to the experimental ones. However, if we take into consideration all the ten modes, then the simulated REPs fit well with those of the experiment, as shown below.

Clark *et al* [36] suggested that the excited state lifetime Γ in most cases is small, and rarely exceeds 0.5ω (ω being frequency in wave numbers of the vibrational mode), but for the two mode calculations a fairly large Γ value has been used. Hence, we carried out

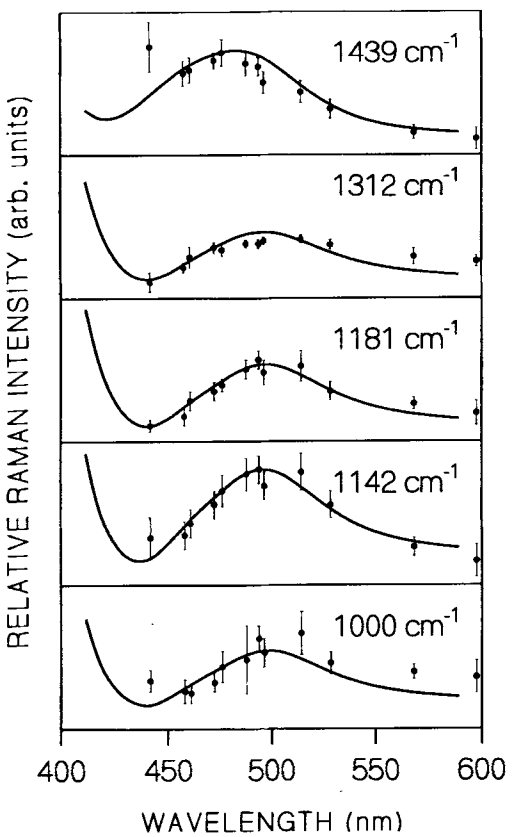

Figure 4. REPs of TAB obtained from multi-mode calculations. Solid lines are the simulated curves and dotted line with error bar shows the experimental curve. $E^{R}_{00} = 20470\ cm^{-1}$ and $E^{I}_{00} = 27710\ cm^{-1}$. Γ is $50\ cm^{-1}$, $M_R = 0.8$Å and $M_I = 2.52$Å.

a multi-mode calculation involving all the ten Raman active totally symmetric modes of TAB in order to simulate the REPs for the five vibrational modes undergoing de-enhancement. Multi-mode simulations not only require small values of Γ but are also much more realistic. The REPs for the modes 1439, 1312, 1181, 1142 and 1000 cm^{-1} are shown in figure 4. The E^{R}_{00} and E^{I}_{00} values for the two electronic states and M_R, M_I are same as that of the two mode calculation. The damping parameter Γ is 50 cm^{-1}. Thus, from figure 4 it can be seen that multi-mode calculations, which include an interfering state, reproduce the experimental REPs well for the five modes undergoing de-enhancement. In figure 4, only the modes that display de-enhancement effects are shown, but simulations have also been carried out for all the ten modes. These compare well with the REPs observed experimentally in terms of the relative intensities, band widths and band positions. For the sake of simplicity, the dimensionless displacements (Δ) for the excited electronic potential energy surfaces of all the totally symmetric vibrations have been taken to be positive, but in reality displacements can be either positive or negative. Further, using the values of Δs, M_R, M_I, E^{R}_{00}, E^{I}_{00} and Γ used in the REP simulation, the absorption spectrum for the ($2^1A_g \leftarrow 1^1A_g$) transition is computed. A comparison of the simulated and the experimental absorption spectrum of TAB in CCl_4 is shown in figure 5. A very good fit of this simulation with the experimental spectrum confirms that the assumptions and parameters used for the REP simulations are valid. In table 2 the vibrational frequencies, their assignments and the simulated displacement values are given. As suggested by Shin and Zink [16], it is seen from table 2 that the five vibrational modes exhibiting de-enhancement do have the expected large Δ_2 values compared to all the other vibrational modes.

This confirms that the de-enhancement effect is caused by the interference due to an electronic state with a transition moment larger than the resonant state. Further, it may be concluded that there is no evidence of a curve crossing between the two electronic states. Since the simulations have been carried out with the symmetry forbidden state as

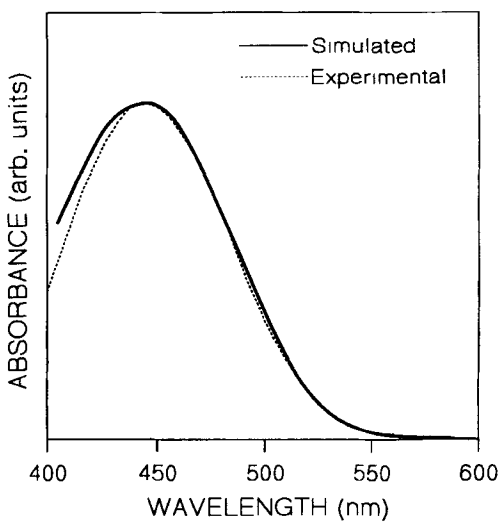

Figure 5. Simulated (————) and experimental (.....) absorption spectrum of *trans*-azobenzene.

Table 2. Description of vibrations of *trans*-azobenzene, their Raman frequencies (ω in cm^{-1}) and respective dimensionless displacements (Δ_1 and Δ_2) in the resonant and interfering electronic states.

Description of vibrations	Frequency (ω in cm^{-1})	Δ_1	Δ_2
C–C–H ben	939	0·47	0·05
ring def	1000	0·60	1·10
C–N str	1142	1·03	1·70
ring H rock, C–C–H ben	1181	0·67	1·45
ring str, N=N str, C–C–H ben	1312	0·28	0·65
N=N str	1439	0·95	0·70
ring str	1470	0·76	0·15
ring str	1491	0·67	0·15
ring str	1592	0·49	0·08

def: deformation, ben: bending, str: stretching. Linear dissociative mode: $\omega = 912\ cm^{-1}$ and slope $\beta = 980\ cm^{-1}$.

Table 3. *Trans*-azobenzene excited state displacements for 1181 cm^{-1} and 1491 cm^{-1} vibrations.

Frequency (ω in cm^{-1})	Two mode		Ten mode	
	Δ_1	Δ_2	Δ_1	Δ_2
1181	1·5	1·45	0·67	1·45
1491	2·0	0·15	0·67	0·15

the resonant electronic state, we infer that the intensities observed are due to pure resonance for all the vibrational modes observed, albeit some of the modes show de-enhancement. However, we note that in order to unequivocally confirm that the intensities are due to resonance, further experiments are being carried out to observe the overtone intensities and also to measure the depolarization ratios.

4. Displacements under de-enhancement

A comparative account of displacements obtained from two mode and ten mode calculations are presented in table 3 for 1181 and 1491 cm^{-1}, respectively. From the table it is evident that simulations taking only two modes into consideration overestimate the dimensionless displacement in the resonant electronic state, and hence the displacement ratios are not maintained in relation to the experimental intensities. We hasten to add that attempts to retain the ratios of the displacements at values same as the ratio of experimental resonant intensities, could not reproduce the experimental REPs very well.

It is recognized, however, that maintaining the ratio of displacements of two modes to be the same in both the excited electronic states has been successfully used by Shin

and Zink [16]. But, in cases like TAB it is not applicable since it is already known that two different types of dynamics (therefore, different ratios of relative Raman intensities for the various vibrational modes) is expected on excitation under the two electronic states in consideration [23–25]. Thus, the displacements for the vibrational modes in the two different electronic states are unlikely to retain the same ratio. Further, even if we assume the same ratio of displacements in both the electronic states, it is not possible to directly relate the two sets of displacements (Δ_1 and Δ_2) to the structural distortions under the single resonant excitation, Individual displacement values, corresponding to a given vibrational mode, in dimensionless units when converted to actual bond length or bond angle changes can give us an idea regarding the distortions experienced by the molecule upon photo-excitation [1–3, 16], The two sets of displacements obtained here for each mode, however, can be used for a qualitative understanding of the extent of displacements of the various vibrational modes in the two electronic states. For example, the modes having large Δ_2 values undergo de-enhancement, suggesting that these modes are dynamically active (structurally distorted) both in ($1^1A_u \leftarrow 1^1A_g$) and ($2^1A_g \leftarrow 1^1A_g$) transitions, but the vibrations with small Δ_2 values undergo no de-enhancement and hence, are expected to be inactive in the ($1^1A_u \leftarrow 1^1A_g$) transition.

In order to quantitatively relate the displacements to dynamics it is neccessary to determine a unique/single value for the displacement for each mode after the influence of an interfering state. Further work is in progress along this direction by treating the interference of the Franck Condon A'-term with the A-term from the ($1^1A_u \leftarrow 1^1A_g$) transition leading to reduced intensity of totally symmetric modes in the region of symmetry forbidden ($2^1A_g \leftarrow 1^1A_g$) transition.

From this theoretical study it is concluded that utilizing time-dependent wave packet calculations, de-enhancement observed in the REPs in resonance with a symmetry forbidden transition can be accounted for as due to interference from a higher energy transition. In spite of its simplicity and accurate description of the de-enhancement effect, the time-dependent approach cannot effectively be used to derive excited state distortions of vibrational modes in which de-enhancement is severe. This is caused by the use of correlation functions in which displacements in both the electronic states are taken into consideration. To study the dynamics in the excited state for vibrational modes involving de-enhancement, it would be realistic to treat vibronic coupling within the same electronic state as the major source of interference.

Acknowledgements

The authors would like to acknowledge the financial assistance from the National Laser Program, Department of Science and Technology, the Council of Scientific and Industrial Research, Government of India and the Jawaharlal Nehru Centre for Advanced Scientific and Industrial Research.

References

[1] A B Myers and R A Mathies, in *Biological Applications of Raman Spectroscopy* edited by T G Spiro (John Wiley and Sons Inc., New York, 1987) vol. 2, p. 1

[2] J I Zink and K-S K Shin, in *Advances in Photochemistry* (John Wiley and Sons Inc., New York, 1991) vol. 16, p. 119

[3] A B Myers, in *Laser Techniques in Chemistry* edited by A B Myers and T R Rizzo (John Wiley and Sons Inc., New York, 1995) vol. 23, p. 325
[4] D L Phillips and A B Myers, *J. Chem. Phys.* **95,** 226 (1991)
[5] F Markel and A B Myers, *J. Chem. Phys.* **98,** 21 (1993)
[6] G A Schick and D F Bocian, *J. Raman Spectrosc.* **11,** 27 (1981)
[7] L A Nafie, R W Pastor, J C Dabrowiak and W H Woodruff, *J. Am. Chem. Soc.* **98,** 8007 (1976)
[8] (a) S P A Fodor, R A Copeland, C A Grygon and T G Spiro, *J. Am. Chem. Soc.* **111,** 5509 (1989)
(b) Y M Bosworth and R J H Clark, *J. Chem. Soc. Dalton Trans.* p. 1749 (1974)
(c) Y M Bosworth, R J H Clark and P C Turtle, *J. Chem. Soc. Dalton Trans.* p. 2027 (1975)
[9] (a) P Stein, V Miskowski, W H Woodruff, J P Griffin, K G Werner, B P Gaber and T G Spiro, *J. Chem. Phys.* **64,** 2159 (1976)
(b) B B Johnson and W L Peticolas, *Ann. Rev. Phys. Chem.* **27,** 465 (1976)
(c) T G Spiro and P Stein, *Ann. Rev. Phys. Chem.* **28,** 501 (1977)
[10] (a) M Z Zgierski, *J. Raman Spectrosc.* **6,** 53 (1977)
(b) M Z Zgierski, *J. Raman Spectrosc.* **5,** 181 (1976)
[11] G M Korenowski, L D Ziegler and A C Albrecht, *J. Chem. Phys.* **68,** 1248 (1978)
[12] S A Asher and C R Johnson, *J. Phys. Chem.* **89,** 1375 (1985)
[13] P Hildebrandt, M Tsuboi and T G Spiro, *J. Phys. Chem.* **94,** 2274 (1990)
[14] W Siebrand and M Z Zgierski, *J. Chem. Phys.* **71,** 3561 (1979)
[15] (a) L Rimai, M E Heyde, H C Heller and D Gill, *Chem. Phys. Lett.* **10,** 207 (1971)
(b) J Friedman and R M Hochstrasser, *Chem. Phys. Lett.* **32,** 414 (1975)
[16] K-S K Shin and J I Zink, *J. Am. Chem. Soc.* **112,** 7148 (1990)
[17] C Reber and J I Zink, *J. Phys. Chem.* **96,** 571 (1992)
[18] I W Sztainbuch and G E Leroi, *J. Chem. Phys.* **93,** 4642 (1990)
[19] H A Kramers and W Heisenberg, *Z. Phys.* **31,** 681 (1925)
[20] P A M Dirac, *Proc. R. Soc. London* **114,** 710 (1927)
[21] A C Albrecht and M C Hutley, *J. Chem. Phys.* **55,** 4438 (1971)
[22] (a) E J Heller, *J. Chem. Phys.* **62,** 1544 (1975)
(b) E J Heller, *J. Chem. Phys.* **68,** 2066 (1978)
(c) K C Kulander and E J Heller, *J. Chem. Phys.* **69,** 2439 (1978)
(d) S-Y Lee and E J Heller, *J. Chem. Phys.* **71,** 4777 (1979)
(e) E J Heller, *Acc. Chem. Res.* **14,** 368 (1981)
(f) A B Myers, R A Mathies, D J Tannor and E J Heller, *J. Chem. Phys.* **77,** 3857 (1982)
(g) D J Tannor and E J Heller, *J. Chem. Phys.* **77,** 202 (1982)
(h) E J Heller, R L Sundberg and D J Tannor, *J. Phys. Chem.* **86,** 1822 (1982)
[23] H Rau, in *Photochromism: Molecules and systems* edited by H Durr and H Bouas-Lauran, (Amsterdam, Elsevier, 1990) p.165
[24] H Rau and S Yu-Quan, *J. Photochem. Photobiol. A: Chemistry* **42,** 321 (1988)
[25] N Biswas and S Umapathy, *Chem. Phys. Lett.* **236,** 24 (1995)
[26] H Okamoto, H Hamaguchi and M Tasumi, *Chem. Phys. Lett.* **130,** 185 (1986)
[27] A B Myers and R A Mathies, *J. Chem. Phys.* **81,** 1552 (1984)
[28] J Tang and A C Albrecht, in *Raman Spectroscopy* edited by H A Szymanski (Plenum, New York, 1970) vol. 2, p. 33
[29] A C Albrecht, *J. Chem. Phys.* **34,** 1476 (1961)
[30] N Biswas, S Umapathy, C Kalyanaraman and N Sathyamurthy, *Proc. Indian Acad. Sci.* **107,** 233 (1995)
[31] R Kosloff, *J. Phys. Chem.* **92,** 2087 (1988)
[32] S O Williams and D G Imre, *J. Phys. Chem.* **92,** 3363 (1988)
[33] M Abramowitz and I A Stegun, *Handbook of Mathematical Function* (Dover, New York, 1968) p. 886
[34] B Tellerer, H H Hacker and J Brandmuller, *Indian. J. Pure Appl. Phys.* **9,** 903 (1971)
[35] S Monti, G Orlandi and P Palmieri, *Chem. Phys.* **71,** 87 (1982)
[36] R J H Clark and T J Dines, *Angew Chem. Int. Ed. Engl.* **25,** 131 (1986)